Journal of the Korean Nuclear Society
Volume 36, Number 1, pp.1 ~ 11, February, 2004

Space Radiation Shielding Calculation by Approximate Model for LEO Satellites

Myung-Won Shin and Myung-Hyun Kim
Kyung Hee University
YongIn-Shi, Gyeongki-do, 449-701, Korea
mwshin@korea.com

(Received February 3, 2003)

Abstract

Two approximate methods for a cosmic radiation shielding calculation in low earth orbits were developed and assessed. Those are a sectoring method and a chord-length distribution method. In order to simulate a change in cosmic radiation environments along the satellite mission trajectory, IGRF model and AP(E)-8 model were used. When the approximate methods were applied, the geometrical model of satellite structure was approximated as one-dimensional slabs, and a pre-calculated dose-depth conversion function was introduced to simplify the dose calculation process. Verification was performed with mission data of KITSAT-1 and the calculated results were also compared with detailed 3-dimensional calculation results using Monte Carlo calculation. Dose results from the approximate methods were conservatively higher than Monte Carlo results, but were lower than experimental data in total dose rate. Differences between calculation and experimental data seem to come from the AP-8 model, for which it is reported that fluxes of proton are underestimated. We confirmed that the developed approximate method can be applied to commercial satellite shielding calculations. It is also found that commercial products of semi-conductors can be damaged due to total ionizing dose under LEO radiation environment. An intensive shielding analysis should be taken into account when commercial devices are used.

Key Words : cosmic radiation, satellite, LEO(low earth orbit), semi-conductor, TID(total ionizing dose), approximate method, shielding

1. Introduction

With the launch of KITSAT-1 and KOREASAT-1 in the early 1990s, domestic satellite industry has begun in Korea. At present, it is scheduled to operate 19 additional satellites by 2015, and to build a launch site for low earth orbit(LEO) satellites by 2005. However, domestic technology level of satellite design is far behind of advanced countries. Space radiation shielding is one of the key items in satellite structure design, because semi-conductor devices, which are susceptible to

high energy cosmic radiation, determine the lifetime and performance of space mission. Therefore, high energy cosmic radiation shielding calculation is an important part of satellite configuration design and risk estimation. Radiation damages in space technology is categorized into three aspects; Single event effect(SEE), displacement damage, Total ionizing dose(TID) effect. TID effect refers to an effect in which the electronic attribute of elements are changed due to cumulative radiation effect that lasts for a long time in semi-conductor elements. It is created when charged particles react with the atoms in elements, and it usually appears in MOSFETs and oxide materials. When a high-energy charged particle enters an MOS(Metal-Oxide Semiconductor) transistor, electron-hole pairs are created in the oxide part. Since an electrons have high mobility, it is easily traced to the electrode, and the holes have very low mobility. Therefore, the holes are trapped by impurities near Si/SiO_2 boundaries, and become a static electric charge. Through the creation of such static electric charge, the electric potential in the transistor deviate from the normal shape. The TID effect takes place at this stage. Since the electronic attributes of the elements such as the threshold voltage and trans-conductor change, the efficiency of semi-conductor devices degrades.

Proton and associated secondary particles are the major sources in shielding calculation for the LEO mission. MCNP-X and LCS (LAHET Code System) are available for this problem of charged particle transport calculation.[1],[2] However, because the calculation time using Monte Carlo codes is too long to describe the radiation environments extremely variable along the orbital path of satellite, these codes have some limitations for space applications. In this study, the effectiveness of approximate methods - sectoring method and chord-length method are evaluated and compared with the results of Monte Carlo calculation and experimental values.

2. Space Radiation Environment Modeling

Shielding calculations are focused on LEO satellite KITSAT-1 whose orbit parameters are shown in Table 1. Most of charged particles on LEO orbit are trapped in an earth geomagnetic field. Therefore, the charged particle flux level at any location is determined by the geomagnetic field strength at that location.[3] In this study, IGRF (International Geomagnetic Reference Field) model[5] is used to calculate geomagnetic field, and AP(E)-8 model[6] is used to calculate charged particle flux spectrum. Figure 1 shows the calculation procedure for shielding calculation in this study. The IGRF model is included in SHELLIG program[7], and the AP(E)-8 model as a

Table 1. Orbit Parameter and Size of KITSAT-1

Orbit Parameter	Value
perigee height (km)	1306.1
apogee height (km)	1326
inclination (degree)	66.08
Size(mm^3)	352 × 356 × 670
Weight (kg)	48.7

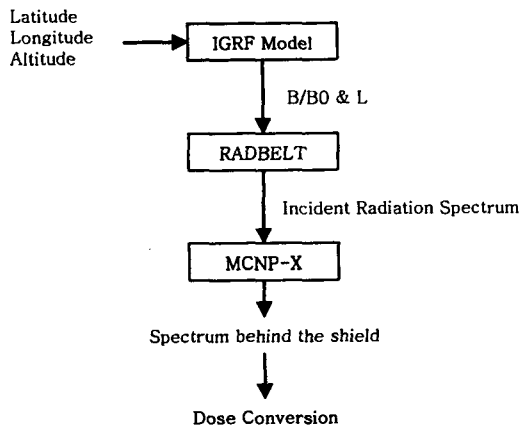

Fig. 1. Code System for Proton Shielding Calculation

library for charged particle flux in RADBELT program[7] is comprised with solar minimum condition and solar maximum condition. In this study, solar minimum condition is applied to shielding calculation.

3. Approximate Shielding Calculation Methods

To determine the shield design, a lot of sensitivity calculations should be performed for shielding structures, locations of semi-conductors and radiation environments. It is impossible to perform all these calculations using the Monte Carlo method. Therefore, it may be an effective alternative to perform the sensitivity study by approximate methods, and then to choose several designs to be further analyzed in detail by the more complex Monte Carlo method.[8] In this study, two approximate methods, the sectoring method and the chord-length method, are used as alternative approaches to Monte Carlo calculations. The complicated satellite structure is described by lots of one dimensional slabs.

When the approximate calculation methods are used, the following two assumptions are applied.

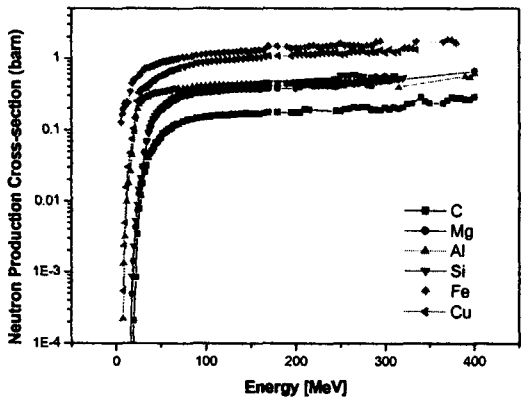

Fig. 2. Cross Section of Secondary Neutron Production Reaction for Various Materials

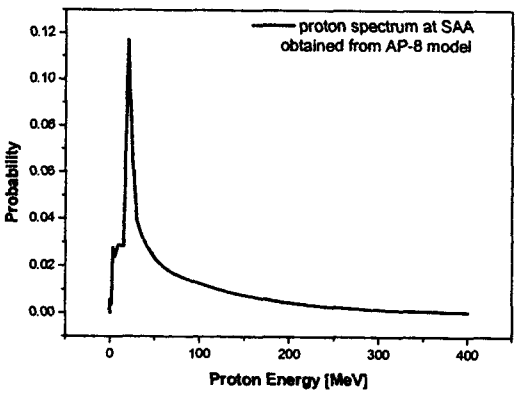

Fig. 3. Calculted Proton Spectrum at SAA Location

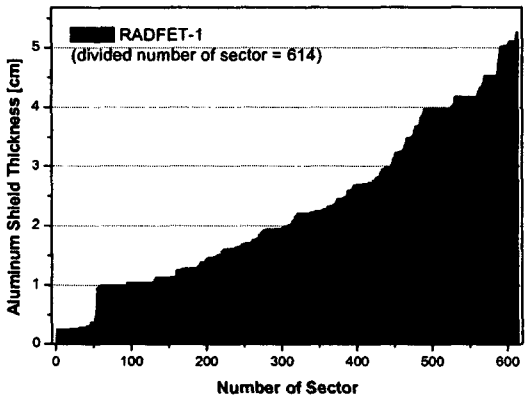

Fig. 4. Shield Thickness Distribution for RADFET-1 in KISAT-1

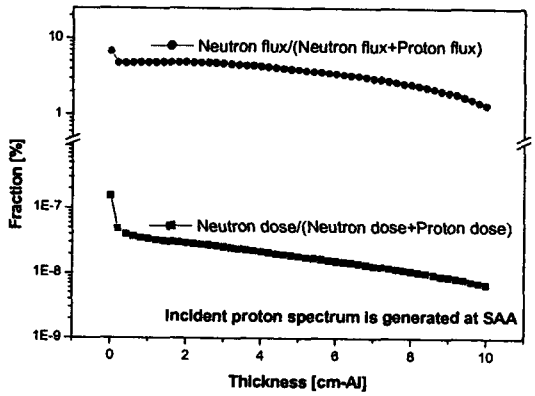

Fig. 5. Secondary Neutron Effect in Al Shield

The first assumption is the deflection of proton in a medium should be neglected. The second assumption is that the effects due to secondary particles are small. As shown in Fig. 2, secondary neutron production reaction cross section is quite low at the range below 50 MeV. Figure 3 which is obtained at SAA area, shows that the proton fluxes having energy beyond 50 MeV are relatively small. Therefore, the reaction rate of secondary neutron production is low. As the shield becomes thicker, the incident proton flux is decreased more at the location in depth, therefore secondary neutron flux is increased. However, the shield thickness of KITSAT-1 is too thin to consider a production of secondary neutron. As shown in Fig. 4, most of the effective shield thickness to target from arbitrary direction is distributed at range below 5 cm. Therefore, most of low energy protons are shielded, and only high energy protons penetrate the shield and interact with semi-conductor directly. As shown in Fig. 5, the effect of secondary neutron is very low and TID effect due to secondary neutron might be negligible. In summary, in LEO space radiation environment, the proton flux having energy enough to produce secondary particle is little, and the shield thickness is not enough to consider secondary particle effect.

It is also assumed in the sectoring method that the charged particles travel in a straight line as an incident ray to a point of interest from the boundary surface locations on divided angle sectors as shown in Fig 6. The thickness of shield in each angular sector is evaluated as a penetrating beam depth along the track direction. Therefore, it is assumed that all of the incident protons to an arbitrary sector penetrate the same distance aluminum. The areal fraction of each sector on the source sphere is used as normalization factor in the dose-rate calculation.

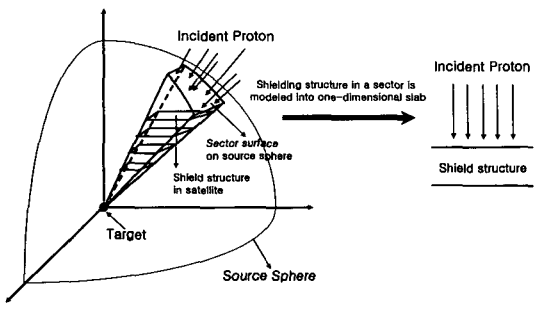

Fig. 6. Examples of Angular Sector Division in a Sectoring Method

Basic steps of the sectoring method to calculate dose at the point of interest are as follows;

① Define the geometry.
② Divide a solid sphere around the point of interest into angular sectors.
③ Calculate the average thickness of material in each sector as viewed from the point of interest.
④ Use the mission dose-depth curve to calculate the dose through the thickness of material for each sector and multiply by the normalization factor.
⑤ Sum the result for each sector to get the total dose estimate for the point of interest.

In the chord-length method, positions of charged particle generation on source boundary is selected arbitrarily by random numbers, and a chord-length is estimated by calculating the effective thickness of shield to a point of interest from each source location. The probability distribution of each chord-length is used as normalization factor when dose-rate is calculated. Basic steps of the chord-length distribution method to calculate dose at the point of interest are as follows;

① Define the geometry.
② Sample the source point on the source sphere.
③ Calculate the shield thickness from the point of interest. (repeat the ② & ③)
④ Calculate chord-length distribution.
⑤ Use the mission dose-depth curve to calculate

the dose through the thickness of material for each chord-length and multiply by the normalization factor.

⑥ Sum the result for each chord-length to get the total dose estimate for the point of interest.

When the proposed approximate method is applied to shielding calculation for satellite, two calculation steps of spectrum calculation and dose conversion should be repeated for each sector and each chord-length by the following two equations.

$$\Phi_g = \sum_{i=0}^{N} [\Phi_g(t_i) \times (N.F.)_i] \quad (1)$$

$$D = \sum_{g=1}^{G} [\Phi_g \times (DCF)_g] \quad (2)$$

In Eq. (1), Φ_g is the charged particle flux at a point of interest with energy group g, $\Phi_g(t_i)$ is the particle flux behind slab thickness t_i with energy group g, and *N.F.* is the normalization factor.

In case of the sectoring method, t_i is the equivalent aluminum thickness of sector *i*, *N* is the number of sector and the areal fraction of sector surface on source sphere is used as *N.F.*

In case of the chord-length method, t_i is the average aluminum thickness of thickness group *i*, *N* is the number of thickness group, and the ratio of number of incident beam penetrating aluminum shield whose thickness is included the in thickness group *i* to the total number of incident particles generated form source surface is used as *N.F.*

In Eq. (2), $\dot{D}$ is the dose rate at a point of interest, and DCF_g is a dose conversion factor at energy group g.

In this study, to enhance the calculation efficiency dose-depth curve is produced in advance using a dose fitting function, $f(t_i)$. This fitting function simplifies the calculation procedure by directly using

$$D = \sum_{g=1}^{G} [D(t_i) \times (N.F.)_i] \quad (3)$$

where $\tilde{D}(t_i)$ is the calculated by using $f(t_i)$, which is a fitting function of dose to thickness.

4. Verification of Approximate Shielding Calculation Method

To verify the effectiveness of approximate methods, two benchmark calculations were performed. Dose rate calculation for a simplified geometry at a constant proton environment was compared with 3-dimensional detailed calculation model. Comparison with experimental values was also evaluated for a limited period of satellite mission.

4.1. Satellite Modeling for Shielding Calculation

KITSAT-1 has the complex structure with stack structures of PCB(printed circuit board) on aluminum and the epoxy package plates as shown in Fig. 7. There are two TID detecting devices, called RADFET-1 and RADFET-3 at DSPE/CRE stack.[9] RADFET-1 is located near the boundary surface and RADFET-3 is at the center of the stack. Since the purpose of this study is to measure the effectiveness of approximate methods, a simple ideal structure of KITSAT-1

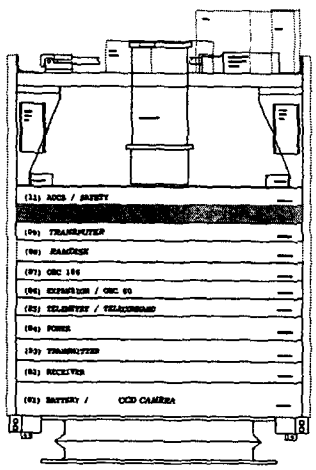

Fig. 7. Configuration of KITSAT-1 Satellite

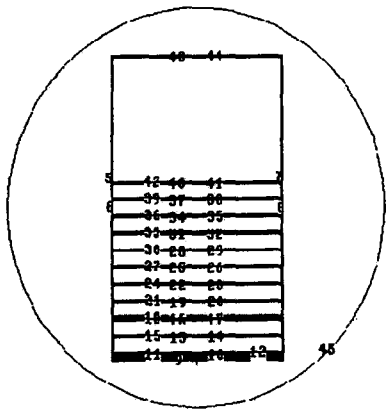

Fig. 8. Calculation Model of KITSAT-1

was modeled with homogeneous material slab of different thickness as shown in Fig. 8. The structured materials were assumed to be aluminum and epoxy only in three-dimensional model calculation. The calculations were performed at two locations, RADFET-1 and RADFET-3 for total dose measurements.

When approximate methods are applied to the shielding calculation, all the structural materials should be converted to reference material, aluminum. Therefore, the thickness of aluminum shield replaced with epoxy is calculated by using averaged stopping power ratio, 0.77.

4.2. Comparison of Approximate Calculation Results with 3-D Detailed Calculation Results

To verify with the results of approximate methods, three-dimensional detailed calculation was performed by using MCNP-X, the transport analysis code for high energy charged particle. The highest source level location at SAA was assumed to be kept with AP-8 model radiation spectrum for this benchmark calculation. Figure 9 shows the proton flux densities at locations of RADFET-1 and RADFET-3.

In the Monte Carlo calculations, the fractional standard deviations in the flux density were less than 1%. The flux at RADFET-1 and RADFET-3 is calculated respectively. The calculated fluxes were converted to dose with the Dose Conversion Factor(DCF) calculated by using stopping power obtained from ICRU(International Commission on Radiation Units and Measurements) Report 49. The dose rates obtained by MCNP-X were 22 mGy/hr at RADFET-1 and 21 mGy/hr at RADFET-3. The difference in dose levels between RADFET-1 and RADFET-3 was insignificant.

As already mentioned, in the approximate methods, dose-depth curve was calculated in advance, and incident proton and electron spectrum were obtained from AP-8 and AE-8 model at SAA. The electron doses including the bremsstrahlung radiation doses were around 1% of proton doses. Therefore, electron dose was neglected to estimate total dose effects in this study. The proton flux behind the thickness of reference material (aluminum) can be calculated by MCNP-X, LAHET and CHARGE. Then the dose-depth curve can be obtained from

$$D(x) = \int_0^{E_{max}} [\ (\mu_a/\rho)(E) \times E \times \phi(x, E) \times C\ ]dE \quad (4)$$

where $\frac{\mu_a}{\rho}$ is mass stopping power of target

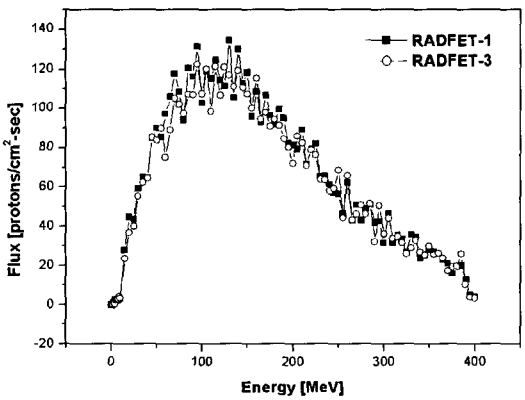

Fig. 9. Calculated Fluxes at Two Locations by MCNP-X Model

material and $\Phi(X,E)$ is proton flux behind the thickness x.

Figure 10 shows the dose-depth curve calculated by the three codes. The values calculated by MCNP-X and LAHET were almost the same up 5 cm thickness aluminum. However, the value calculated by CHARGE was lower than those from the other codes. This difference seems to be generated by the difference in calculation methods and dose conversion factors applied. In case of MCNP-X and LAHET, the dose conversion factors were calculated using stopping power data from ICRU Report49. Although two codes solve a transport equation, CHARGE describes integral behaviors of particles by using the simplified attenuation formula[11]

$$\Phi(E) = \Phi_0(E) \times e^{-\Sigma_{N.E.}(E) \cdot t} \quad (5)$$

where $\Phi_0(E)$ is the incident proton flux and $\Sigma_{N.E.}(E)$ is the proton non-elastic scattering cross section of shield material.

In this study, dose-depth curves used in Eq. 3 is pre-calculated by MCNP-X. Figure 11 shows the result of fitting of the calculated dose-depth curve. We used a second order exponential decay function as the fitting function to be applied.

$$f(x) = 25.42e^{-x/0.29} + 2.53e^{-x/5.96} \quad (6)$$

In the calculation model for sectoring method, satellite space was divided by from 14 to 2,522 angular sectors around the point of interest. For a chord-length method, 1,000,000 random points of source were selected on the source surface which is an external spherical boundary. The line-of-sight thickness from a source position to a point of interest was classified into from 20 to 150 thickness groups. Figure 12 shows dose rates from two approximate methods and 3-D detailed calculation. As the number of sectors and the

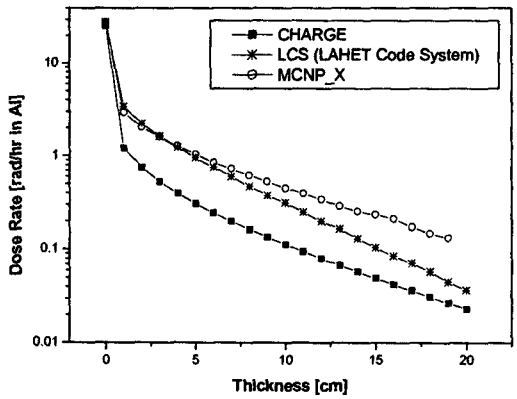

Fig. 10. Dose-Depth Curves for Aluminum at SAA Location

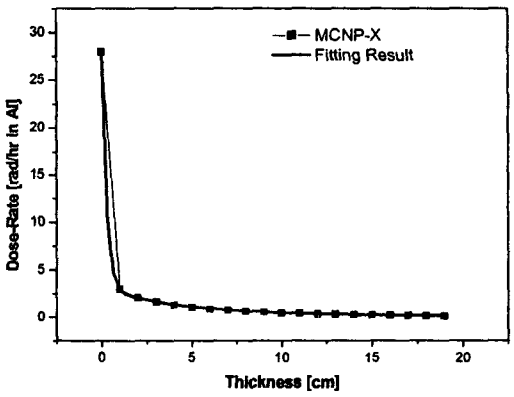

Fig. 11. Fitting Curve for Dose-Depth Conversion (with Proton Spectrum at SAA)

number of thickness group increase, the dose rate results are stabilized. The calculated dose rate and location effect of RADFET-1 and RADFET-3 are shown in Table 2. The dose rate and location effect estimated by approximate method was well agreed with detailed calculation result. The calculated dose by approximate method was overestimated about 15 % for sectoring method and 8 % for chord-length method than 3-D detailed calculation results. Error in approximate method seems to be caused by material conversion error to reference material and by inaccuracy in geometrical satellite modeling.

Table 2. Comparison of Calculated Dose Rates from Three Methods

	RADFET-1	RADFET-3	Relative error between two location (%)
3-D detailed calculation (MCNP-X) (mGy/hr in Al)	22 ± 2.6	21 ± 2.5	4.6
Sectoring Method (mGy/hr in Al)	26	24	6.0
Chord-length Method (mGy/hr in Al)	24	23	4.5

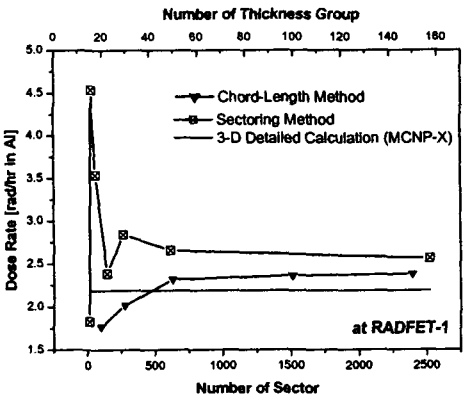

(a) for RADFET-1

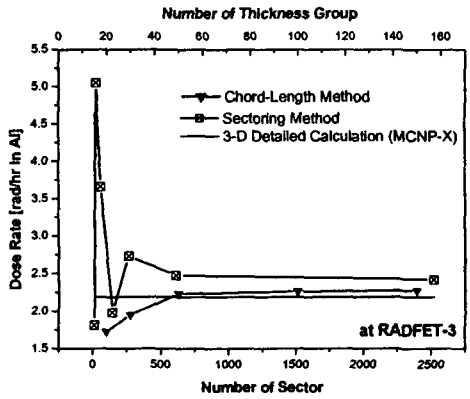

(b) for RADFET-3

Fig. 12. Comparison of Results from Approximate Methods and 3-D Detailed Model

4.3. Comparison of Calculation Results with Experimental Value

The RADFET installed on KITSAT-1 sparks static movements of threshold voltage when that is irradiated. Then, the ground base station receives the information on the movement of threshold voltage from the satellite. Ground experiments are conducted in order to convert the movement of threshold voltage into the radiation dose. The ground experiment was supervised by the Satellite Technology Research Center(SaTReC) of the KAIST, and they used Co-60 gamma ray research equipment in Korea Atomic Energy Research Institute. Since Co-60 gamma ray emits photons with 1.17MeV and 1.33MeV, it can be considered as emitting 1.25MeV photons on the average. 1.25MeV photons transfer energy to mediums through compton scattering, and it has similar effects like high-energy eletrons and protons. Therefore, they are frequently used as the radiation sources for ground experiment in cosmic radiation environments with low radiation. The experiment was performed with 900 Gy(SiO_2)/hr Co-60 gamma ray, and it also utilized the same RADFET as that installed on the KITSAT-1 which is a modified p-channel MOSFET.[9] Using the result of the experiment, SaTReC converted the threshold voltage after one year period(1992.9 - 1993.8) into dose values for RADFET-1 and RADFET-3. The results were 7.7 mGy(SiO_2)/day and 5.7 mGy(SiO_2)/day, respectively. To compare

Table 3. Comparison of Calculated Dose Rate with Experimental Data

	at RADFET-1 location	at RADFET-3 location	Relative error between two location (%)
Experimental Data (mGy/hr in SiO2)	7.7	5.7	78.2
Sectoring Method (mGy/hr in SiO2)	3.9	2.8	39.3
Chord-Length Method (mGy/hr in SiO2)	2.7	2.4	12.5

Fig. 13. Orbit of KITSAT-1 Used in Simulation

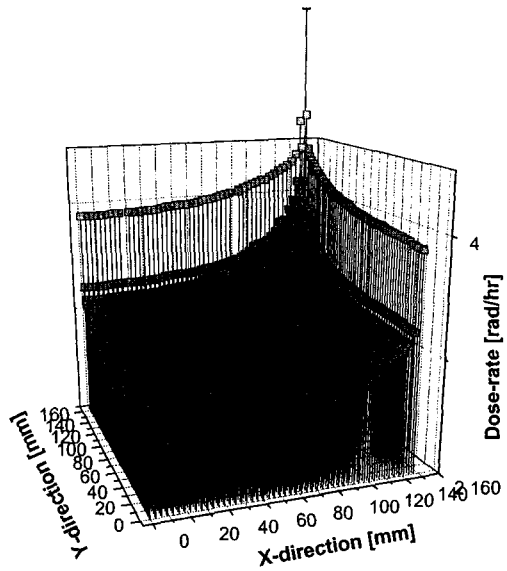

Fig. 14. Calculated Dose Rate Distribution on SDPE/CRE Stack (with SAA Spectrum)

with experimental value, shielding calcuation should be performed at the satellite at points along its orbital path because radiation environments vary. Therefore, in this study, the time averaged proton flux was calculated and applied as a constant cosmic radiation environment. In order to compare with experimental value, orbital operation condition of KITSAT-1 was simulated as shown in Fig. 13. The averaged proton flux spectrum was obtained from simulation for a period of about 1 month operation. The dose-depth curve is calculated from averaged proton spectrum, and fitting function was also calculated. Calculation results and experimental values were compared in Table 3.

In case of mission simulation under condition, location effect of RADFET-1 and RADFET-3 was larger than using proton spectrum at SAA. Calculation results were lower than experimental values.

The reasons for the discrepancy includes the experimental process, satellite modelling, radiation environment modeling and others. Among them, the biggest reason is that AP-8, the radiation environment model, was not quite reliable and the effects of temperature change were not taken into account. Recent analysis from data of several satellites shows that the AP-8 model underestimated the accumulated radiation dose by

Table 4. Total Dose Test Results for Various Commercial(CMOS) ICs

Part Type	Dose Rate (Gy/hr)	Test Ckt	Failure Level
32 bit DSP	1.26 - 1.69	Emulator	50 Gy
128KX8 RAM (Hitachi)	2.41 - 18.0	APG Board	50 Gy
386 μP (INTEL)	0.40 - 0.61	Std. Board	75 Gy
32KX8 Seeq EEPROM	0.68 - 1.30	Std. Board	150 Gy
4-Ch MUX (Harris)	0.40 - 2.60	Std. Board	> 300 Gy
32KX8 RAM (Hitachi)	2.48 - 10.01	Std. Board	200 Gy

some 40 %. This result is consistent with the result of recent satellite data analysis[12],[13] as well as the result of the calculation using APEXRAD model using APEX satellite(1993, 1000km, 70 degree).[12] AP(E)-8 model was developed based on data from 1960s, therefore, it might have had significant errors in data for cosmic radiation environments.

5. Shielding Calculation for KISAT-1 with Sectioring Method

To analyze a geometrical effects in shielding for KITSAT-1, TID values are calculated on every location of SDPE/CRE stack by using a sectoring method. KITSAT-1 is divided by 2,525 angular sectors ($\Delta\vartheta$=5°, $\Delta\varphi$=5° in spherical geometry), and TID is calculated at 2,750 locations on SDPE/CRE stacks. As shown in Fig. 14, shielding effects are very different at every locations in satellite. The dose-rates at RADFET-1 and RADFET-3 are 26 mGy/hr and 24 mGy/hr respectively under SAA radiation environment. The maximum value in dose rate was larger about 250% than the minimum value in a single panel. Therefore, because the shielding effect is largely variable with the location of semi-conductor in satellite, the location effect should be considered in satellite configuration design.

In table 4, the failure levels of commercial semi-conductors are compared.[14] The average TID value of functional failure is about 105 Gy.

The operation period of KITSAT-1 was designed to be about 5 years(1992.9-1996.10). If the radiation environment at SAA is applied conservatively, the TID values at RADFET-1 and RADFET-3 are 1139 Gy and 1051 Gy respectively. When a time-averaged proton spectrum is applied along the mission track, TID values are 144 Gy and 124 Gy respectively. This result shows that even under LEO condition, some of commercial semi-conductor devices can not stand upto their lifetime in satellite without an additional shielding design. In addition to this fact, a solar condition should be considered in AP-8 model, the risk of failure due to TID, then, might be much higher.

6. Conclusions

In this study, two approximate calculation methods for shielding calculation of cosmic radiation were developed and assessed. For a verification of the two approximate methods,

three dimensional Monte-Carlo calculation result and ground experiment result were compared with. The approximate calculation methods evaluated total dose conservatively at two detector locations within a satellite structure. However, approximate methods underestimated total dose compared with experimental data. It was found that selection of location in a structure might be another crucial design point with the thickness of the shield around the device. It was also found that commercial semi-conductors can be damaged due to TID effect even in LEO condition.

References

1. R.E. Prael, & H. Lichtenstein, *User Guide to LCS: The Lahet Code System*, p.5-20, Los Alamos National Laboratory, New Mexico(1989).
2. L.S. Waters, *MCNPX Users Manual, Version 2.1.5*, p.15-54., Los Alamos National Laboratory, New Mexico(1999).
3. J. Barth, *Modeling Space Environment*, in IEEE NSREC Short Courses, pp.22-48, IEEE Publishing Services, New Jersey(1997).
4. J.W. Haffner, *Radiation and Shielding in Space*, p. 107-175, Academic Press, New York(1967).
5. C.E. Barton, "International Geomagnetic Reference Field:Seventh Generation," J. Geomagnetic & Geoelectric, Vol. 49, p.123-148, (1997).
6. D.W. Sawyer and J.I. Vette, Ap-8 Trapped Proton Environment for Solar Maximum and Minimum, NSSDC/WDC-A-R&S 76-06, (1976).
7. J.I. Vette, The NASA/National Space Data Center Trapped Radiation Environment Model Program(1964-1991), NSSDC/WDC-R&S 91-29, (1991).
8. J.D. Kinnison, *Achieving Reliable, Affordable Systems*, in IEEE NSREC Short Courses, p.14-16, IEEE Publishing Services, New Jersey(1998).
9. S.J. Kim, Y.H. Shin, & K.W. Min, "Simulation of Shielding Effects on The Total Dose Observed in TDE of KITSAT-1," *Journal of Astronomy and Space Sciences*, 18, 71-80 (2001).
10. M.W. Shin & M.H. Kim, "Comparison of Approximate Models for High Energy Cosmic Radiation Shielding Calculation," *Journal of Astronomy and Space Sciences*, 19, p.151-162 (2002).
11. W.R. Yucker & J. R. Lilley, *CHARGE Code for Space Radiation Shielding Analysis*, p.6-24, McDonnell Douglas Astronautics Co., California(1969).
12. Gussenhoven, M. S., Mullen, E. G., Bell, J. T., Madden, D. & Holeman, E, APEXRAD: low altitude orbit dose as a function of inclination, magnetic activity and solar cycle, IEEE Transactions on Nuclear Science, Vol. 44, 1997.
13. Petersen, E. L. Predictions and observations of SEU rates in space, IEEE Transactions on Nuclear Science, Vol. 44, 1997.
14. Space Radiation Effects Handbook, p.3-7, Space Radiation Inc.(1997).